

Endovascular aneurysm repair alters renal artery movement: a preliminary evaluation using dynamic CTA.

6

Bart E. Muhs MD¹, Arno Teutelink MD¹, Matthias Prokop MD, PhD², Koen L. Vinciken PhD², Frans L. Moll MD, PhD¹, Hence J.M. Verhagen MD, PhD¹

Departments of Vascular Surgery¹ and Radiology². University Medical Center, Utrecht, the Netherlands

J Endovasc Ther. 2006 Aug;13(4):476-80.

Abstract

Introduction:

It is unclear what comprises natural renal artery motion per cardiac cycle in patients with AAAs, and how the implantation of stent-grafts may distort this movement. We studied these phenomena dynamically using EKG-gated 64-slice CTA.

Methods:

Fifteen patients (29 renal arteries) were studied, 6 pre- and 9 post-EVAR. Pre-EVAR scans represented normal renal artery motion in patients with aneurysms. The post-EVAR scan was used to study the effect of endografts. Data was acquired using an EKG-gated dynamic 64-slice CT scanner during a single breath hold. Eight gated data sets, covering the cardiac cycle were reconstructed, perpendicular to the center flow lumen of each renal artery at 1.2cm and 2.4cm from aortic attachment. Center of mass displacement was determined per cardiac cycle for pre- and post-EVAR renal arteries. Pre- and post-EVAR renal movements were compared using a students T-test with $p=0.05$ considered significant.

Results:

Normal renal artery motion in AAA patients is impressive with up to 3mm movement both near and distant from the aorta (range 1.1mm3.0mm, mean 2.0mm, SD 0.57mm). EVAR inhibits proximal renal motion resulting a 31% decrease in maximal movement (range 0.69mm2.0mm, mean 1.4mm, SD 0.7mm)($p=0.05$). Distal renal artery motion is unaffected by EVAR with motion similar to the pre-EVAR state.

Conclusion:

EKG-gated dynamic CTA is feasible on a 64-slice scanner with a standard radiation dose and can detect potentially serious consequences of EVAR. EVAR alters renal artery motion by limiting proximal cardiac cycle motion while leaving distal motion unaffected.

Introduction

The traditional pre- and post-operative sizing and measurements of endografts for the treatment of infrarenal abdominal aortic aneurysms (AAA) have been carried out using static contrast enhanced computerized tomography angiography (CTA)¹⁻⁴. EVAR results in substantial static changes in aneurysm and aortic morphology with a reported 15% increase in neck angulation and 27% decrease in neck length in large AAAs treated via endovascular means⁵. We hypothesized that morphologic renal artery alterations might be observed when subjected to altered mechanical forces following EVAR. Utilizing dynamic CTA as a new diagnostic tool, small renal artery changes per cardiac cycle can be recorded and measured in addition to the larger static changes of the aorta and aneurysm sac following EVAR. The human aorta and its renal sidebranches are part of a dynamic, pulsatile environment. Alteration in renal artery dynamics may be involved in disease states, including intimal hyperplasia, renal artery stenosis, and atherosclerosis and have implications for future endograft designs^{6, 7}. Little attention has been given to renal artery motion per cardiac cycle in patients with infrarenal aneurysms or the consequences of EVAR on this motion. Recent reports are beginning to evaluate normal renal artery motion⁸⁻¹⁰. Three-dimensional analysis of renal artery bending during respiration using contrast enhanced magnetic resonance angiography (CE-MRA) has shown maximum displacements of 13.2 mm between inspiration and expiration⁹. The use of breath hold techniques can minimize respiration induced renal artery motion, but normal arterial pulsatility during the cardiac cycle can also produce motion.

The purpose of this study was to utilize 64-slice EKG-gated cine-CT scanning to characterize pre-operative renal artery motion in AAA patients during the cardiac cycle. Furthermore, we evaluated the post-operative effect of EVAR on renal artery motion.

Methods

Patients were evaluated at a single institution for AAA repair. All patients were male. Indication for EVAR and determination of endograft device was made by the surgeon. EVAR was performed by one operating surgeon. CT scans used for analysis were obtained as part of the standard pre- and post-operative evaluation protocol. Not all patients evaluated had both pre- and post-operative scans. Patients were not subjected to additional CT scanning or radiation exposure.

Fifteen patients with 29 renal arteries were studied, six pre- and nine post-EVAR using either the Talent (n=6) or Excluder (n=3) device. Data was acquired using an EKG-gated dynamic 64-slice CT scanner (Philips Medical Systems, Cleveland, OH, USA). Images were acquired during a single breath-hold phase of 20 seconds during which the entire abdomen was imaged. The imaging protocol was set at

1.25 mm collimation and a pitch of 0.25. Radiation exposure parameters were 120 kVp and 300 mAs, resulting in a CT dose index ($CTDI_{vol}$) of 21 mGy. Intravascular non-ionic contrast (120 ml) (Imerol 300, Schering, Berlin, Germany) followed by a 50ml of saline chaser bolus was injected at a flow rate of 4ml/s. The scan was started using bolus triggering software with a threshold of 100HU over baseline. EKG triggered retrospective reconstructions were made at eight equidistant time points over the R-R cardiac cycle. The data set of each patient was loaded into a separate workstation (Extended Brilliance Workspace, Philips Medical Systems, Cleveland, OH, USA) and processed using the cardiac review program function. The gated data sets, covering the cardiac cycle, were reconstructed perpendicular to the center flow lumen of each renal artery at 1.2 cm and 2.4 cm from aortic attachment (i.e. renal ostia) (Figure 1). The renal ostia served as the reference point for the 1.2 cm and 2.4 cm measurements. The measurements were taken in relation to the reference point at each time point during the cardiac cycle. Center of mass (COM) was plotted on a Cartesian coordinate system and maximal COM displacement determined per cardiac cycle for pre- and post-EVAR renal arteries. Both pre- and post-EVAR renal movement was determined and compared using a Students T-test with $p=0.05$ considered significant.

Results

Image acquisition was accomplished in all scanned patients with image quality rated as good to excellent. Renal artery motion in patients with infrarenal aneurysms is impressive with up to 3 mm maximal movement both near and distant from the aorta (range 1.1 mm 3.0 mm, mean 2.0 mm, SD 0.57 mm) (Figure 2). Maximal COM displacement did not necessarily occur in the anterior-posterior or sagittal plane. Renal artery motion exists in a three dimensional (3D) environment with complex movement and conformation changes. EVAR with suprarenal fixation significantly inhibits proximal physiologic renal motion resulting a 31% decrease in maximal movement (range 0.69 mm 2.0 mm, mean 1.4 mm, SD 0.7 mm)($p=0.05$)(Figure 3). Distal renal artery motion is unaffected by EVAR with motion similar to the pre-EVAR state (Figure 4). Both pre- and post-EVAR renal arteries typically exhibit a 'figure of eight' direction of movement (Figure 5).

Discussion

We report pre-operative renal artery motion of 1 mm to 3 mm in proximal (1.2 cm) and distal (2.4 cm) locations along the renal artery in patients with infrarenal aneurysms. With up to 3 mm movement per cardiac cycle occurring over millions of heart beats, it is conceivable that renal artery movement may play a causative role in renal artery stent fractures^{6, 7}.

Multiple authors have reported on the renal function following EVAR¹¹⁻¹⁶. Although

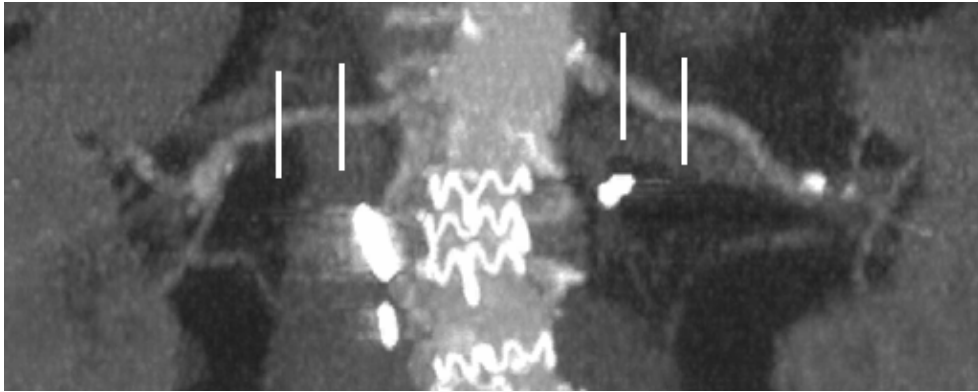


Figure 1.
Sagittal static CTA demonstrating with lines illustrating the level at which measurements were made on dynamic cine-CT images. Measurements were taken at 1.2 cm and 2.4 cm from the renal artery aortic origin.

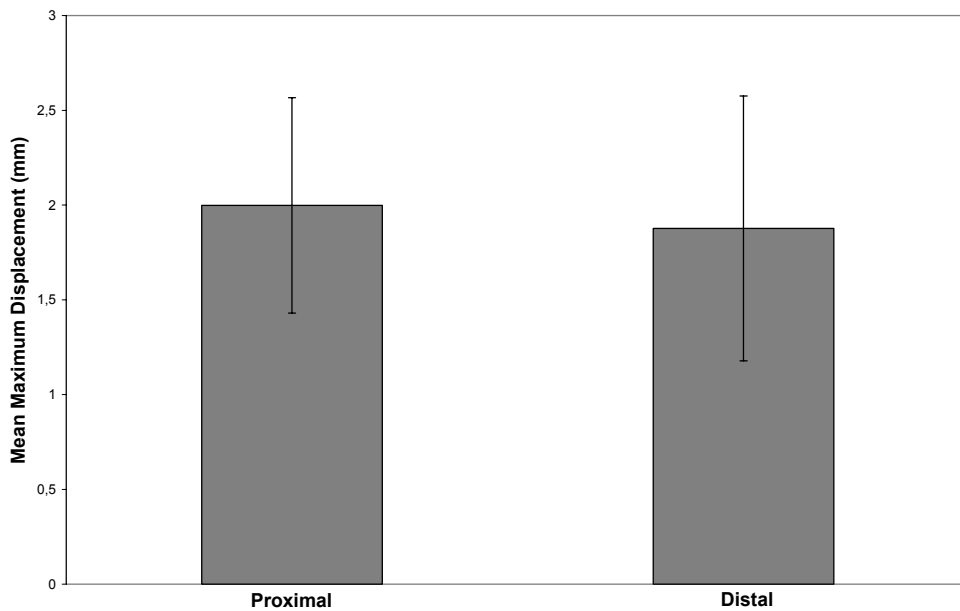


Figure 2.
Mean maximum COM displacement at 1.2 cm and 2.4 cm during the cardiac cycle in patients with AAAs prior to EVAR. There is no difference in COM movement between these two levels ($p=NS$).

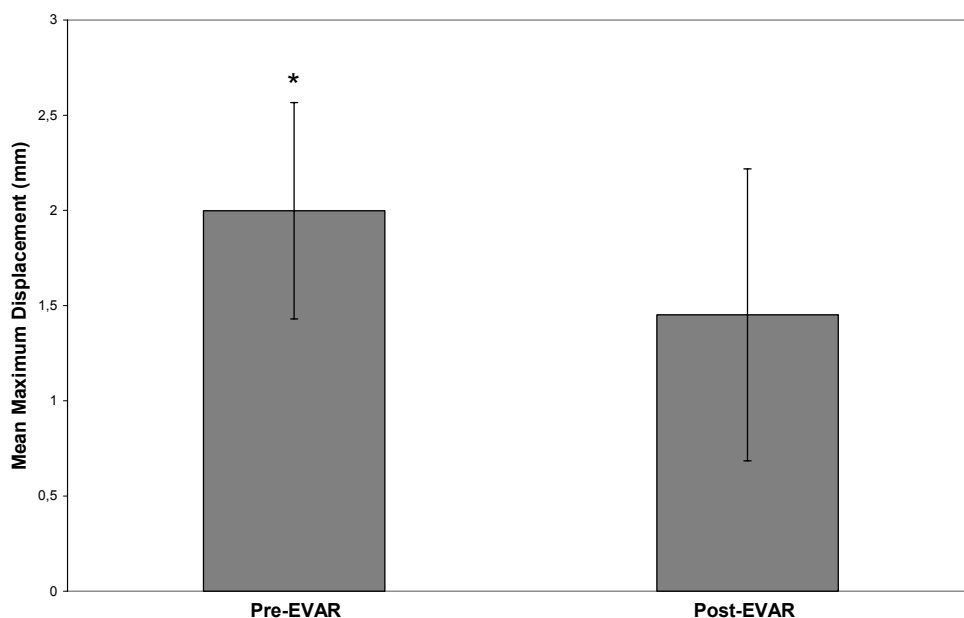


Figure 3. Mean maximum COM displacement at 1.2 cm pre- and post-EVAR during the cardiac cycle. There is a significant decrease in COM movement following EVAR ($p < 0.05$).

our study did not examine renal function, we demonstrated that the presence of an endograft has dynamic consequences for the renal arteries. Whether or not this has functional implications remains unknown at this time. This preliminary study was designed to determine if EVAR effected pre-operative renal motion and was not powered to determine differences between stentgraft designs. Future studies evaluating potential differences between stentgrafts are anticipated.

We have shown with our study that EVAR alters renal artery motion only at the 1.2 cm point. However, 2.4 cm from the renal artery ostium, renal artery motion is unaffected by EVAR. Changes in angles, bending, and complex (3D) changes in configuration are taking place. Perhaps, the presence of a relatively stiff device placed adjacent to a moving renal artery 'pins' the proximal renal artery, thus limiting motion while the more distal renal artery is of sufficient distance from the endograft to minimize its motion limiting effect. We selected 1.2 cm and 2.4 cm distances based on previous reports and our preliminary analysis of maximal motion. We also selected these distances because they are relevant anatomic points for fenestrated and branched endografts which are emerging as complex AAA treatment options.

Renal fenestrated and branched endografts typically employ renal stents less

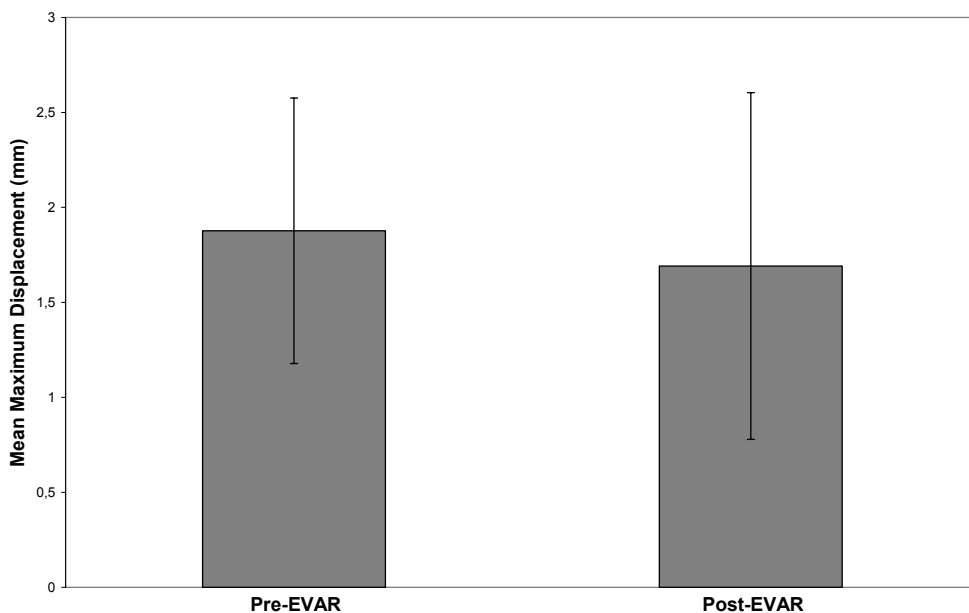


Figure 4.
 Mean maximum COM displacement at 2.4 cm pre- and post-EVAR during the cardiac cycle. There is no difference in movement at this level following EVAR ($p=NS$).

than 2.4 cm but greater than 1.2 cm in length^{17, 18}. The end point of a renal stent in these complex cases would fall somewhere between this reports' measured distances and within a maximal area of arterial conformational change. Endografts with stiff renal sidebranches may result in further alteration of renal artery motions. The consequences on renal stent durability, progression or initiation of renal disease, and potential for endoleaks are unknown. However, concern is raised by this preliminary report. This concern is strengthened by early reports of significant renal insufficiency following fenestrated endografting^{19, 20}.

In conclusion, EKG-gated dynamic CTA is feasible on a 64-slice scanner and provides insight into renal motion before and after EVAR. EVAR appears to change renal artery movement by limiting proximal cardiac cycle renal artery motion while leaving distal motion unaffected. Any ill consequences of these complex dynamic renal artery changes are presently unknown, but with fenestrated and branched procedures emerging, issues of stent durability, fixation systems, and long-term renal artery effects should be considered.

References

1. Gomes, M.N., W.J. Davros, and R.K. Zeman, *Preoperative assessment of abdominal aortic aneurysm: the value of helical and three-dimensional computed tomography*. J Vasc Surg, 1994. **20**(3): p. 367-75; discussion 375-6.
2. Filis, K.A., F.R. Arko, G.D. Rubin, et al., *Three-dimensional CT evaluation for endovascular abdominal aortic aneurysm repair. Quantitative assessment of the infrarenal aortic neck*. Acta Chir Belg, 2003. **103**(1): p. 81-6.
3. Siegel, M.J., *Multiphase and three-dimensional multi-detector row CT of thoracic vessels and airways in the pediatric population*. Radiology, 2003. **229**(3): p. 641-50.
4. Rubin, G.D., A.J. Schmidt, L.J. Logan, et al., *Multi-detector row CT angiography of lower extremity arterial inflow and runoff: initial experience*. Radiology, 2001. **221**(1): p. 146-58.
5. Arko, F.R., K.A. Filis, B.B. Hill, et al., *Morphologic changes and outcome following endovascular abdominal aortic aneurysm repair as a function of aneurysm size*. Arch Surg, 2003. **138**(6): p. 651-5; discussion 655-6.
6. Bessias, N., G. Sfyroeras, K.G. Moulakakis, et al., *Renal artery thrombosis caused by stent fracture in a single kidney patient*. J Endovasc Ther, 2005. **12**(4): p. 516-20.
7. Sahin, S., A. Memis, M. Parildar, et al., *Fracture of a renal artery stent due to mobile kidney*. Cardiovasc Intervent Radiol, 2005. **28**(5): p. 683-5.
8. Vasbinder, G.B., J.H. Maki, R.J. Nijenhuis, et al., *Motion of the distal renal artery during three-dimensional contrast-enhanced breath-hold MRA*. J Magn Reson Imaging, 2002. **16**(6): p. 685-96.
9. Draney, M.T., C.K. Zarins, and C.A. Taylor, *Three-dimensional analysis of renal artery bending motion during respiration*. J Endovasc Ther, 2005. **12**(3): p. 380-6.
10. Kaandorp, D.W., G.B. Vasbinder, M.W. de Haan, et al., *Motion of the proximal renal artery during the cardiac cycle*. J Magn Reson Imaging, 2000. **12**(6): p. 924-8.
11. Malina, M., M. Lindh, K. Ivancev, et al., *The effect of endovascular aortic stents placed across the renal arteries*. Eur J Vasc Endovasc Surg, 1997. **13**(2): p. 207-13.
12. Malina, M., J. Brunkwall, K. Ivancev, et al., *Renal arteries covered by aortic stents: clinical experience from endovascular grafting of aortic aneurysms*. Eur J Vasc Endovasc Surg, 1997. **14**(2): p. 109-13.
13. Mehta, M., N. Cayne, F.J. Veith, et al., *Relationship of proximal fixation to renal dysfunction in patients undergoing endovascular aneurysm repair*. J Cardiovasc Surg (Torino), 2004. **45**(4): p. 367-74.
14. Lobato, A.C., R.C. Quick, P.L. Vaughn, et al., *Transrenal fixation of aortic endo-*

- grafts: intermediate follow-up of a single-center experience.* J Endovasc Ther, 2000. **7**(4): p. 273-8.
15. Alric, P., R.J. Hinchliffe, M.C. Picot, et al., *Long-term renal function following endovascular aneurysm repair with infrarenal and suprarenal aortic stent-grafts.* J Endovasc Ther, 2003. **10**(3): p. 397-405.
 16. Greenberg, R.K., T.A. Chuter, M. Lawrence-Brown, et al., *Analysis of renal function after aneurysm repair with a device using suprarenal fixation (Zenith AAA Endovascular Graft) in contrast to open surgical repair.* J Vasc Surg, 2004. **39**(6): p. 1219-28.
 17. Verhoeven, E.L., T.R. Prins, I.F. Tielliu, et al., *Treatment of short-necked infrarenal aortic aneurysms with fenestrated stent-grafts: short-term results.* Eur J Vasc Endovasc Surg, 2004. **27**(5): p. 477-83.
 18. Greenberg, R.K., S. Haulon, S. O'Neill, et al., *Primary endovascular repair of juxtarenal aneurysms with fenestrated endovascular grafting.* Eur J Vasc Endovasc Surg, 2004. **27**(5): p. 484-91.
 19. Haddad, F., R.K. Greenberg, E. Walker, et al., *Fenestrated endovascular grafting: The renal side of the story.* J Vasc Surg, 2005. **41**(2): p. 181-90.
 20. Greenberg, R.K., S. Haulon, S.P. Lyden, et al., *Endovascular management of juxtarenal aneurysms with fenestrated endovascular grafting.* J Vasc Surg, 2004. **39**(2): p. 279-87.

